Am J Transl Res 2026;18(3):1972-1985
www.ajtr.org /ISSN:1943-8141/AJTR0168555

Original Article

Swept-source optical coherence tomography quantitative scoring system accurately predicts postoperative intraocular pressure control and visual outcomes in primary angle-closure glaucoma

Huaifeng Li, Zhen Yao

Department of Ophthalmology Ward 2, Liuyang Jili Hospital, Liuyang City, Changsha 410300, Hunan, China

Received September 4, 2025; Accepted December 25, 2025; Epub March 15, 2026; Published March 30, 2026

Abstract: Objective: To evaluate the clinical utility of the swept-source optical coherence tomography (SS-OCT) scoring system in the long-term management of primary angle-closure glaucoma (PACG). Methods: Clinical data of 136 PACG patients (155 eyes) who underwent phacoemulsification combined with goniosynechialysis between June 2021 and July 2023 were retrospectively analyzed. Based on intraocular pressure (IOP) one year postoperatively, patients were categorized into a controlled group (IOP < 21 mmHg, 85 patients, 98 eyes) and an uncontrolled group (IOP ≥ 21 mmHg, 51 patients, 57 eyes). SS-OCT was used to assess retinal nerve fiber layer (RNFL) thickness, optic disc parameters, Schlemm's canal morphology, angle opening distance at 500 μm (AOD500), trabecular-iris angle at 500 μm, and visual acuity. Logistic regression analysis was performed to identify factors influencing postoperative IOP control. Results: The uncontrolled group showed higher IOP and lower RNFL thickness than the controlled group ($P < 0.05$). After treatment, the uncontrolled group exhibited higher cup-to-disc area ratio and diameter ratios than the controlled group ($P < 0.05$). Schlemm's canal diameter (SCD), Schlemm's canal area (SCA), and AOD500 were significantly lower in the uncontrolled group both before and after treatment ($P < 0.05$). Pre-treatment IOP was negatively correlated with SCD, SCA, and AOD500 ($r < 0$, $P < 0.05$). Elevated IOP was identified as a risk factor for postoperative IOP control in PACG patients ($OR > 1$, $P < 0.05$). Conclusion: The SS-OCT scoring system accurately quantifies postoperative IOP control, RNFL thickness, optic disc parameters, and visual function changes in PACG patients, providing guidance for personalized treatment.

Keywords: Swept-source optical coherence tomography, primary angle-closure glaucoma, retinal nerve fiber layer, optic disc parameters, Schlemm's canal morphology, intraocular pressure control

Introduction

Primary angle-closure glaucoma (PACG) is one of the most prevalent forms of glaucoma. According to the international classification, primary angle-closure disease (PACD) is divided into three clinical entities, including PACG, primary angle closure (PAC), and primary angle-closure suspect (PACS), according to disease severity. Epidemiological data indicate that by 2040, Asia is expected to bear the highest global burden of PACD [1]. Its pathogenesis primarily involves progressive narrowing or closure of the anterior chamber angle, impeding aqueous humor outflow, thereby elevating intraocular pressure (IOP) and leading to the loss of retinal ganglion cells (RGCs) and irreversible optic nerve damage [2]. Without timely intervention during the early or remission stages, 40%-80% of PACG patients may experience acute episodes within 5-10 years, accelerating visual function deterioration [3]. Although anterior chamber angle morphology, aqueous humor outflow function, and retinal nerve fiber layer (RNFL) thickness are closely associated with PACG progression, few studies have investigated the relationship between postoperative restoration of Schlemm's canal (SC) morphology and RNFL preservation [4].

Currently, PACG is primarily treated surgically in clinical practice. Phacoemulsification combined

https://doi.org/10.62347/PIKB3348

with goniosynechialysis (phaco-GSL) facilitates aqueous humor outflow and reduces IOP by removing the crystalline lens and releasing synechiae in the anterior chamber angle. However, postoperative IOP control remains unsatisfactory in some patients, and the absence of effective postoperative monitoring indicators and predictive methods affects the long-term efficacy assessment [5]. Traditional clinical follow-up mostly relies on single indicators such as IOP and visual acuity, which fails to fully reflect the dynamic changes in anterior chamber angle, SC morphology, and optic nerve injury. Optical coherence tomography (OCT) is a high-resolution, non-invasive imaging modality capable of providing micron-level cross-sectional images of the retina and choroid, playing an important role in the early detection and disease characterization of glaucoma [6]. Swept-source optical coherence tomography (SS-OCT) further improves imaging precision, enabling non-invasive and dynamic visualization of the optic disc, RNFL, SC, and postoperative changes [7]. In addition, the unique advantage of SS-OCT lies in its ability to non-invasively and clearly visualize the structural details of the anterior chamber angle (such as the trabecular meshwork, Schlemm's canal status, and peripheral iris morphology) and the choroidal structure. Existing studies indicate that SS-OCT provides objective imaging data for PACG diagnosis and assessing structural and functional remodeling following glaucoma surgery; however, its application in postoperative efficacy assessment and long-term follow-up remains rarely reported [8].

Based on this rationale, the present study hypothesizes that the SS-OCT quantitative scoring system can accurately assess postoperative changes in IOP, SC morphology, and optic nerve structure in patients with PACG. Key SS-OCT-derived parameters, including Schlemm's canal diameter (SCD), Schlemm's canal area (SCA), and angle opening distance at 500 μm (AOD500), are expected to be closely associated with postoperative IOP control and may serve as predictors of surgical outcomes. Therefore, this study aims to quantitatively analyze the dynamic changes in structural and functional parameters before and after surgery in PACG patients using SS-OCT, and to construct a predictive model for postoperative IOP control, thereby providing objective evidence for individualized follow-up and risk assessment.

Materials and methods

From June 2021 to July 2023, clinical data of 136 patients with PACG, involving a total of 155 eyes, were retrospectively analyzed. All patients underwent phaco-GSL. This study was approved by the Ethics Committee of Liuyang Jili Hospital [Approval No. HA202501]. Due to the retrospective nature, all data were obtained from anonymized medical records and imaging data, with the exemption of individual informed consent granted by the Ethics Committee of Liuyang Jili Hospital.

Inclusion criteria: (1) a diagnosis of PACG according to the Expert Consensus on Diagnosis and Treatment of Primary Glaucoma in China (2014) [9]; (2) meeting the corresponding surgical indications for phaco-GSL; (3) complete clinical and postoperative follow-up data; (4) eligibility for SS-OCT examination, with good image quality.

Exclusion criteria: (1) a history of ocular surgery (e.g., cataract surgery, glaucoma surgery); (2) presence with lens dislocation or subluxation affecting aqueous humor outflow; (3) diagnosis with non-PACG types of glaucoma (including chronic open-angle glaucoma, secondary glaucoma, and traumatic glaucoma); (4) prior laser treatment (e.g., YAG laser peripheral iridotomy, selective laser trabeculoplasty); (5) severe preoperative visual impairment (visual field loss greater than 50%); (6) significant media opacity (e.g., grade II or higher cataract, corneal opacity, vitreous opacity); (7) other disorders of fundus (e.g., optic neuritis, diabetic retinopathy); (8) severe systemic diseases (e.g., malignant hypertension, end-stage renal disease); (9) congenital fundus disorders; (10) poor imaging quality (inability to obtain clear measurements of critical structures using SS-OCT).

Intervention methods

All patients underwent phaco-GSL. Preoperatively, the conjunctival sac was irrigated, followed by disinfection and sterile draping. A lid speculum was applied, and local anesthesia was administered. A clear corneal incision was made at the superotemporal quadrant of the affected eye, with an auxiliary side incision at the 2 o'clock position. Sodium hyaluronate gel was injected into the anterior chamber via the side incision, followed by goniosynechialysis. A gonioscope was placed to systematically ex-

amine the entire anterior chamber angle (0°-360°) to determine the location and extent of the angle adhesion. The blunt goniotomy device was inserted into the anterior chamber. Under direct gonioscope vision, the tip of the device was gently inserted into the target quadrant of the angle recess, kept close to the anterior surface of the trabecular meshwork, and blunt separation was performed along the contour of the iris root. Adequate separation was considered achieved when the SC was clearly visualized and aqueous humor outflow was unobstructed, with the range of separation covering at least 180°. Lens nucleus and cortex were separated. The lens nucleus was fragmented and aspirated using a phacoemulsification system. Residual cortex was cleared with an irrigation/aspiration handpiece, and the posterior capsule and anterior chamber were polished. Sodium hyaluronate gel was injected with an injection-aspiration needle to gently press the iris root, achieving blunt dissection of the anterior chamber angle, thereby confirming angle opening and unobstructed aqueous humor outflow. The gel was subsequently aspirated, the incision was closed, and the procedure was concluded. In the event of anterior chamber hemorrhage or corneal edema during surgery, anterior chamber irrigation and flushing were performed.

Postoperative medications: All patients were administered routine antibiotics and corticosteroid eye drops. Specifically, 0.1% fluorometholone eye drops were administered four times daily for 2 weeks, and levofloxacin eye drops were administered four times daily for 1 week. In approximately 25% patients with early postoperative elevated IOP, timolol eye drops were administered twice daily or latanoprost eye drops were administered once daily until the IOP returned to normal. Postoperative medication regimens were identical in all patients to control for the potential confounding effects of medication.

Data collection and indicator definitions

Follow-up examinations were arranged at 1, 3, and 6 months postoperatively. However, data were missing for some patients during early follow-up, resulting in incomplete short-term data. As the study focused on long-term structural and functional changes after PACG, the 1-year postoperative data demonstrated the highest coverage and best represented the stable postoperative state. Therefore, complete preoperative and 1-year postoperative data were ultimately selected for analysis. Short-term follow-up data were used for clinical monitoring but were not involved in the main statistical analysis.

Data collection methods

IOP was measured using a non-contact tonometer, and the average of three measurements was taken. SS-OCT examinations were performed by the same experienced technician to ensure reproducibility.

SS-OCT parameters

All parameters were automatically measured and manually calibrated using a SS-OCT system (DRI OCT Triton). SCD refers to the maximum internal diameter of SC in cross-section; SCA refers to the total area enclosed by the lumen of SC in cross-section; AOD500 refers to the distance from the anterior surface of the trabecular meshwork to the posterior surface of the cornea, 500 μm from the scleral spur; RNFL thickness: the average thickness of the macula and optic disc periphery, calculated using the automated layer segmentation algorithm of the SS-OCT system; Optic disc parameters include cup-to-disc ratio (C/D ratio), rim area (RA), and cup area (CA).

IOP measurement and grouping methods

All patients underwent IOP measurements at a fixed time (8:00-10:00 AM) to minimize the influence of circadian fluctuations. Measurements were taken using a Goldmann applanation tonometer. During measurement, patients were seated to avoid Valsalva-induced IOP variations. After routine instillation of topical anesthetic (0.5% proparacaine) and staining with sodium fluorescein, measurements were performed by the operator using a slit lamp microscope. For each patient, IOP was measured three consecutive times by the same ophthalmologist, and the average value was calculated as the raw IOP of that visit. If the coefficient of variation (CV) of the three measurements exceeded 10%, the measurement was considered invalid. After a 5-minute rest, another three consecutive measurements were performed by the same ophthalmologist. All IOP measurements were corrected according to the central corneal thickness using the built-in

calibration procedure of tonometer. To ensure data reliability, the procedure was conducted independently by two ophthalmologists, with cross-validation to enhance data reliability. All SS-OCT scans and baseline IOP measurements were completed within 1 week before the scheduled surgery. During this period, patients either did not receive any IOP-lowering medications or were in a stable state after a washout period. According to the Glaucoma Guidelines of the Chinese Ophthalmological Society (2021), an IOP of 21 mmHg is considered the critical threshold for postoperative IOP control. Therefore, based on the corrected IOP values and medication use obtained at the 1-year follow-up (12 months ± 1 month after surgery), patients were categorized into two groups:

Controlled group included patients whose IOP was less than 21 mmHg at one year postoperatively, without the need for IOP-lowering medication.

Uncontrolled group included those whose IOP ≥ 21 mmHg at one year postoperatively or who required IOP-lowering medication for maintenance.

SS-OCT examination

The DRI SS-OCT system (Topcon, Japan) was used for imaging. The parameters were set as follows: a maximum resolution of 512 × 256, a light source wavelength of 1,050 nm, a scanning range of 12 mm × 9 mm, and a scanning speed of 100,000 scans per second. Patients were instructed to fixate on the internal target light to maintain ocular stability. The operator adjusted the scanning position to ensure comprehensive coverage of the target regions, including the optic disc and RNFL. The scan was initiated with the optic disc as the center, performing a circular retinal scan within a 3 mm radius. The operator switched the scan mode to the anterior segment scan module. The scan position was adjusted to focus on the limbus (usually in the nasal or temporal quadrant) to clearly visualize the anterior chamber angle structures, including the iris root, trabecular meshwork, scleral protuberance, and SC, ensuring that the scan line or scan area covered the target angle structures. The SS-OCT image analysis system was utilized to generate quantitative assessments of RNFL thickness (global, superior, and inferior), optic disc parameters [CA, disc area (DA), RA, rim volume (RV), and cup volume (CV)], SC morphology (SCD, SCA), AOD500, and trabecular-iris angle at 500 μm (TIA500). The optic disc parameters were generated automatically or semi-automatically from the three-dimensional volume scan data centered on the optic disc. The operator may need to manually correct the optic disc boundary markers; however, all primary quantitative analyses were performed automatically by the software.

Outcome measures

The primary outcome measures included the postoperative IOP reduction and the success rate of postoperative IOP control. The secondary outcome measures included changes in SS-OCT structural parameters (SCD, SCA, AOD500, RNFL thickness, C/D ratio), trends in SS-OCT quantitative scores, and adverse events (postoperative IOP elevation, corneal edema, etc.).

Data quality control

All imaging data were analyzed independently by two examiners, each with at least five years of experience in image interpretation. Any discrepancies exceeding 5% were reviewed by a third expert, and the average value was taken. All data were entered into the database using a double-entry method to ensure accuracy.

Data analysis

Statistical analysis was conducted using SPSS 25.0. Continuous data were expressed as mean ± standard deviation (mean ± SD). Paired-samples t-tests were used for comparisons within groups before and after treatment, while independent-samples t-tests were used for comparisons between groups. Categorical data were presented as percentages and analyzed using the χ^2 test. Pearson correlation analysis was conducted to analyze the correlation between research variables. To investigate the relationship between preoperative indicators and postoperative IOP control, a multivariable logistic regression model was established, with postoperative IOP control as the dependent variable (0 = controlled, 1 = uncontrolled) and preoperative indicators with statistical differences (IOP, SCD, SCA, AOD500, all continuous variables) as independent variables. Since the original regression coefficient of AOD500 was relatively large, indicating scale differenc-

Table 1. Comparison of baseline characteristics between the two groups

Variable	Controlled group (n = 85, 98 eyes)	Uncontrolled group (n = 51, 57 eyes)	t/χ^2	*P*
Age (years, χ ± s)	58.9 ± 4.7	57.8 ± 5.2	1.26	0.21
Sex (male/female, cases)	40/45 (47.06%/52.94%)	23/28 (45.10%/54.90%)	0.05	0.82
BMI (kg/m^2)	23.15 ± 2.18	22.98 ± 2.07	0.45	0.65
Disease duration (years)	25.88 ± 2.75	26.98 ± 3.87	1.80	0.074

Note: BMI: body mass index.

es from other variables, Z-score standardization was applied to AOD500 before establishing the logistic regression model to minimize the impact of dimensional disparity on model stability. The stepwise method was used to select variables included in the final model, and the adjusted regression coefficients, odds ratios (OR), and their 95% confidence intervals (95% CI) were calculated. The independent variables were examined using the variance inflation factor (VIF), with VIF > 10 indicating the presence of multicollinearity. $P < 0.05$ was considered statistically significant.

Results

Demographic and clinical characteristics of the patients

A total of 136 patients (155 eyes) with PACG who underwent phaco-GSL were included in this study. The patients comprised 63 males and 73 females, aged 32-78 years, with a mean age of (58.3 ± 4.9) years. The mean body mass index (BMI) was (23.09 ± 2.12) kg/m^2, and the mean disease duration was (26.5 ± 3.5) years.

Among them, 85 patients (98 eyes, 62.5%) were assigned to the controlled group, and 51 patients (57 eyes, 37.5%) to the uncontrolled group. The mean age was (58.9 ± 4.7) years in the controlled group and (57.8 ± 5.2) years in the uncontrolled group, with no significant difference ($P > 0.05$). In terms of sex distribution, the controlled group included 40 males (47.06%) and 45 females (52.94%), while the uncontrolled group included 23 males (45.10%) and 28 females (54.90%), with no significant difference ($P > 0.05$). The BMI was (23.15 ± 2.18) kg/m^2 in the controlled group and (22.98 ± 2.07) kg/m^2 in the uncontrolled group (P > 0.05). The disease duration was (25.88 ± 2.75) years in the controlled group and (26.98 ± 3.87) years in the uncontrolled group ($P > 0.05$). These data indicate that the baseline characteristics of the two groups were comparable (**Table 1**).

RNFL thickness parameters

The global, superior, and inferior RNFL thicknesses did not differ significantly between the two groups before treatment ($P > 0.05$). After treatment, the global, superior, and inferior RNFL thicknesses in the uncontrolled group were significantly declined compared to before treatment ($P < 0.05$) and were notably lower than those in the controlled group ($P < 0.05$), indicating that structural damage to the RNFL was more pronounced in the uncontrolled group. The RNFL thickness in the controlled group remained stable compared to preoperative values ($P > 0.05$), indicating better postoperative structural recovery (**Figure 1**).

Optic disc parameters and morphological characteristics of SC

The uncontrolled group demonstrated significantly larger C/D ratio and smaller RA and RV compared with the controlled group ($P < 0.05$), indicating incomplete recovery of optic disc structure. After treatment, both groups demonstrated significant increases in SCD and SCA ($P < 0.05$). Among them, SCD in the controlled group increased from (121.48 ± 20.68) μm preoperatively to (168.26 ± 23.35) μm postoperatively, while in the uncontrolled group, it increased from (103.25 ± 18.57) μm to (141.49 ± 22.18) μm. SCA in the controlled group increased from (3680.59 ± 561.05) μm^2 preoperatively to (5348.59 ± 885.98) μm^2, while in the uncontrolled group, it increased from (2635.87 ± 487.49) μm^2 to (4746.65 ± 684.15) μm^2. Compared with the uncontrolled group, the controlled group demonstrated significantly greater improvement in postoperative SCD and SCA (both $P < 0.05$), suggesting that effective IOP control is more closely associated with structural expansion of SC. However,

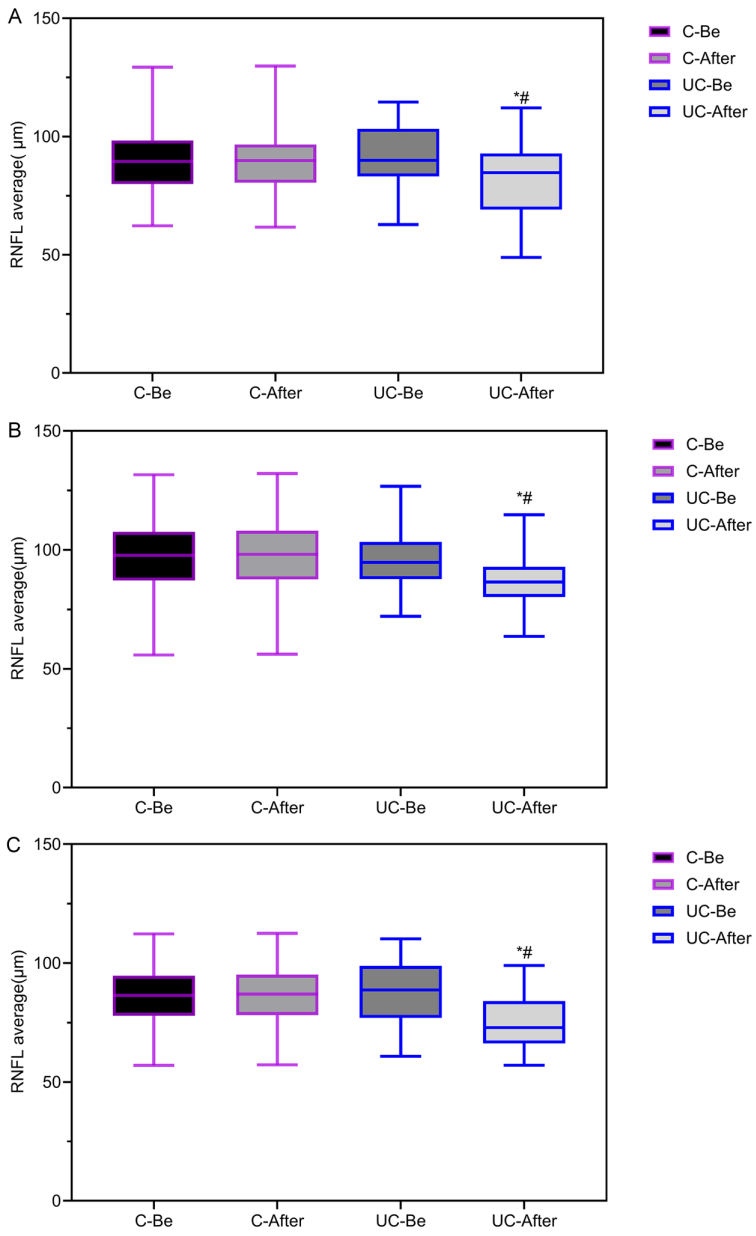

Figure 1. Comparison of RNFL thickness between the controlled and uncontrolled groups before treatment and one year after treatment. A: Global RNFL thickness; B: Superior RNFL thickness; C: Inferior RNFL thickness. C-Be: controlled group before treatment; C-After: controlled group after treatment; UC-Be: uncontrolled group before treatment; UC-After: uncontrolled group after treatment; RNFL: retinal nerve fiber layer. One year after treatment, the RNFL thickness remained largely stable in the controlled group, whereas a significant reduction was observed in the uncontrolled group compared with before treatment. Compared with the same group before treatment, $^{*}P < 0.05$; compared with the controlled group at the same time point, $^{\#}P < 0.05$.

Figure 2 presents the OCT findings of a representative case from the uncontrolled group. The patient's both eyes exhibited asymmetry in RNFL thickness. In the right eye (OD), the peripapillary RNFL showed a continuous structure, and the thickness curve remained within the normal reference range without evidence of focal thinning. In the left eye (OS), the OCT showed an irregular RNFL profile, large fluctuations in the thickness curve, and a trend toward structural disruptions in local areas, indicating a risk of RNFL damage. The OCT showed that the RNFL boundaries in the OS were less well-defined than in the OD, with heterogeneous reflectivity suggesting reduced structural stability. Interocular asymmetry analysis indicated a difference between OD and OS, further supporting the possibility of unilateral structural abnormality.

Comparison of TIA500 and AOD500 between the two groups

Before treatment, the uncontrolled group exhibited significantly lower AOD500 and TIA500 values than the controlled group ($P < 0.05$). After treatment, both parameters increased significantly in the two groups ($P < 0.001$). However, the uncontrolled group demonstrated lower postoperative AOD500 and TIA500 values than the controlled group ($P < 0.05$), suggesting incomplete anterior chamber angle opening in patients with poor IOP control (**Figure 3**).

the increase was smaller in the uncontrolled group ($P < 0.05$), indicating a limited improvement in aqueous humor outflow function (**Table 2**). In addition, to further illustrate the typical characteristics of RNFL thickness changes,

Correlation analysis between pre-treatment IOP and SS-OCT parameters

Pearson correlation analysis revealed that pre-treatment IOP was significantly negatively cor-

Table 2. Comparison of optic disc parameters between the controlled and uncontrolled groups

Parameters	Controlled group (n = 98)		Uncontrolled group (n = 57)	
	Before treatment	After treatment	Before treatment	After treatment
C/D ratio	0.52 ± 0.12	0.48 ± 0.15	0.54 ± 0.11	0.55 ± 0.13$^{###}$
Horizontal C/D diameter ratio	0.60 ± 0.15	0.48 ± 0.15	0.61 ± 0.19	0.62 ± 0.18$^{###}$
Vertical C/D diameter ratio	0.54 ± 0.12	0.42 ± 0.1	0.53 ± 0.14	0.56 ± 0.15$^{###}$
DA (mm^2)	2.51 ± 0.32	2.52 ± 0.29	2.53 ± 0.38	2.67 ± 0.38$^{***,###}$
CA (mm^2)	1.32 ± 0.25	1.34 ± 0.28	1.31 ± 0.29	1.35 ± 0.31
RA (mm^2)	1.08 ± 0.29	1.11 ± 0.31	1.21 ± 0.30	0.99 ± 0.28$^{***,###}$
RV (mm^2)	0.18 ± 0.08	0.17 ± 0.06	0.17 ± 0.07	0.12 ± 0.05$^{***,###}$
CV (mm^2)	0.45 ± 0.09	0.48 ± 0.11	0.44 ± 0.10	0.45 ± 0.11
SCD (μm)	121.48 ± 20.68	168.26 ± 23.35***	103.25 ± 18.57$^{###}$	141.49 ± 22.18$^{***,###}$
SCA ($μm^2$)	3680.59 ± 561.05	5348.59 ± 885.98***	2635.87 ± 487.49$^{###}$	4746.65 ± 684.15$^{***,###}$

Note: C/D: cup-to-disc; DA: disc area; CA: cup area; RA: rim area; RV: rim volume; CV: cup volume; SCD: Schlemm's canal diameter; SCA: Schlemm's canal area. Compared within the same group before treatment, $^{***}P < 0.001$; compared with the controlled group at the same time point, $^{###}P < 0.001$.

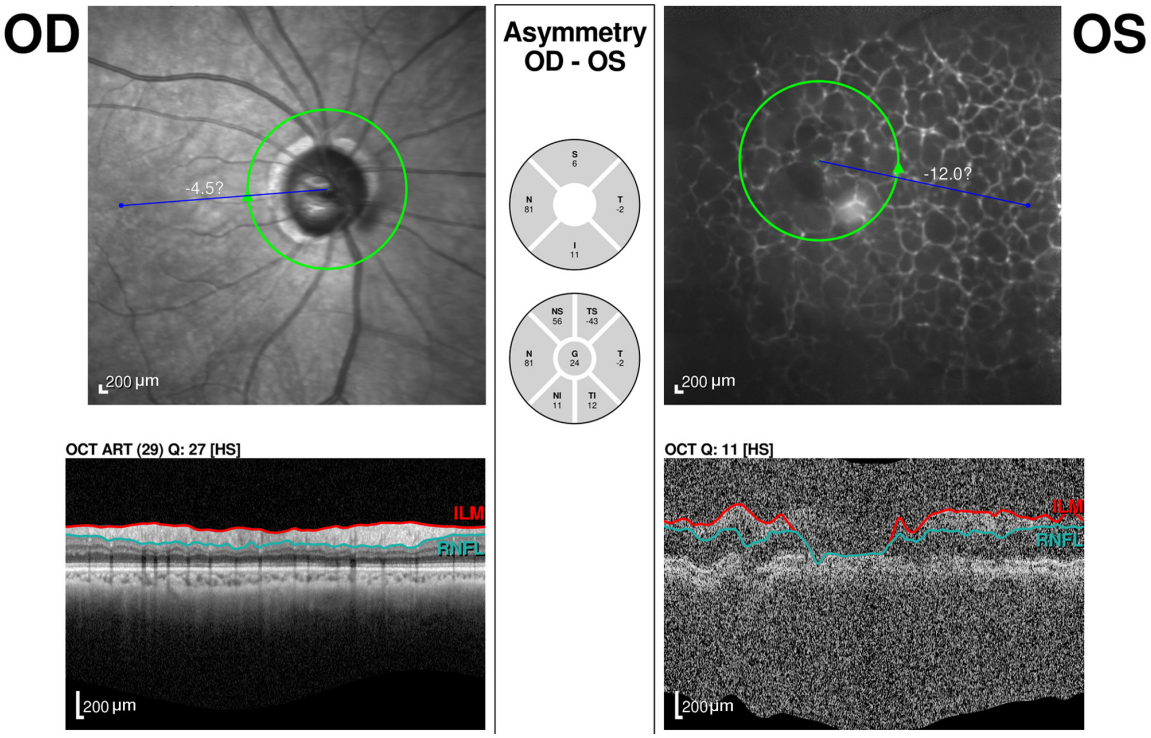

Figure 2. A representative case in the uncontrolled group. Note: The patient's both eyes exhibited asymmetry in RNFL thickness. In the right eye (OD), the RNFL structure was relatively intact, with the thickness curve remained within the normal reference range. The left eye (OS) exhibited localized fluctuations and mild thinning in the RNFL thickness profile, which may indicate early structural changes. These imaging findings were consistent with the overall trend of RNFL thinning observed in the uncontrolled group of this study. RNFL: retinal nerve fiber layer.

related with SCD (r = -0.208, P = 0.010), SCA (r = -0.402, P < 0.001), and AOD500 (r = -0.268, P = 0.001). Specifically, smaller SCD, SCA, and angle-opening distance were associated with higher IOP, suggesting a close relationship between abnormal anterior chamber angle structure and elevated IOP (**Figure 4**).

Analysis of factors influencing postoperative IOP control in PACG patients

Logistic regression analysis revealed that elevated preoperative IOP was identified as an independent risk factor for poor postoperative IOP control in PACG patients (B = 0.271, OR =

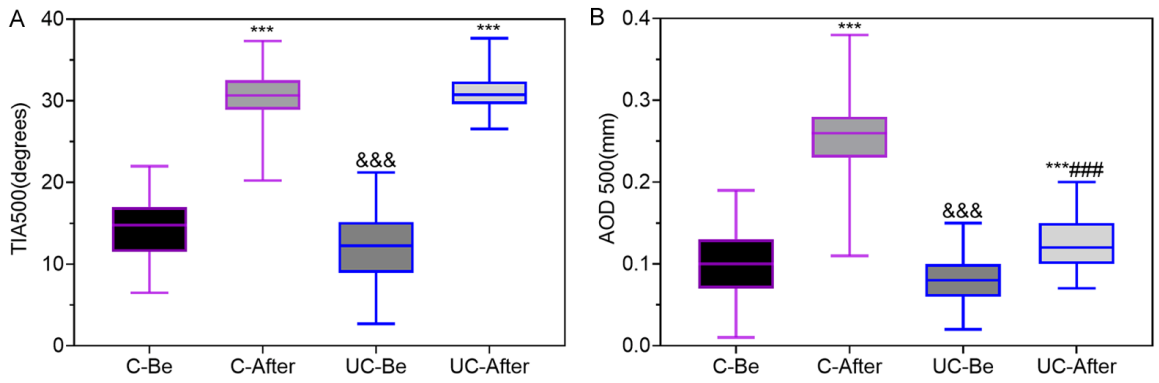

Figure 3. Comparison of TIA500 and AOD500 between the controlled and uncontrolled groups. A: TIA500; B: AOD500. Note: C-Be: controlled group before treatment; C-After: controlled group after treatment; UC-Be: uncontrolled group before treatment; UC-After: uncontrolled group after treatment; TIA500: trabecular-iris angle at 500 μm; AOD500: angle opening distance at 500 μm. Compared with the same group before treatment, $^{***}P < 0.001$; compared with the controlled group after treatment, $^{\#\#\#}P < 0.001$; compared with the controlled group before treatment, $^{\&\&\&}P < 0.01$.

1.311, 95% CI: 1.112-1.546, $P = 0.001$). Among the anterior chamber angle parameters, SCD, SCA and AOD500 all exerted protective effects on postoperative IOP control, with AOD500 demonstrating the most pronounced protective effect. After standardization, AOD500 remained in the final model (B = -1.705, OR = 0.182, 95% CI: 0.072-0.459, $P < 0.001$), indicating that a decrease in AOD500 significantly increased the risk of poor postoperative IOP control.

In addition, SCD (B = -0.036, OR = 0.965, 95% CI: 0.935-0.996, $P = 0.028$) and SCA (B = -0.004, OR = 0.996, 95% CI: 0.995-0.998, $P < 0.001$) exhibited statistical significance despite smaller ORs, indicating that even minor improvements in anterior chamber angle parameters may reduce the likelihood of poor postoperative IOP control (**Table 3**).

ROC curve analysis results

The ROC analysis showed that preoperative IOP had strong predictive ability, with an AUC of 0.826 (95% CI: 0.757-0.894, $P < 0.001$), indicating good discriminatory power for postoperative IOP control status. In comparison, the AUC values for SCD (AUC = 0.741, 95% CI: 0.663-0.820, $P < 0.001$), SCA (AUC = 0.921, 95% CI: 0.880-0.961, $P < 0.001$) and AOD500 (AUC = 0.797, 95% CI: 0.727-0.866, $P < 0.001$) were all greater than 0.5, indicating that these anterior chamber angle parameters also possessed good predictive capability. Among these parameters, SCA exhibited the highest AUC (0.921), suggesting that it may have greater diagnostic value in predicting postoperative IOP control. It should be noted that the AUC for the combined indicator was 0.923 (95% CI: 0.883-0.963, $P < 0.001$), indicating that the predictive ability of the multi-parameter combined model was superior to that of any single indicators (**Figure 5**).

Postoperative adverse reactions

The postoperative adverse reactions of the two groups of patients were systematically evaluated. During the early postoperative period (1 day to 1 week postoperatively), transient IOP elevation occurred in 8 cases (8.2%) in the controlled group and 7 cases (12.3%) in the uncontrolled group, with no significant difference between groups ($P = 0.39$). Corneal edema occurred in 5 cases (5.1%) in the controlled group and 4 cases (7.0%) in the uncontrolled group ($P = 0.60$). Mild anterior chamber hemorrhage was observed in 3 cases (3.1%) in the controlled group and 2 cases (3.5%) in the uncontrolled group ($P = 0.88$). The recurrence rate of synechia was also low, with 2 cases (2.0%) in the controlled group and 2 cases (3.5%) in the uncontrolled group ($P = 0.58$). All adverse reactions were mild and resolved within a short period after routine management.

During the 1-year postoperative follow-up, neither group of patients experienced long-term complications such as persistent corneal

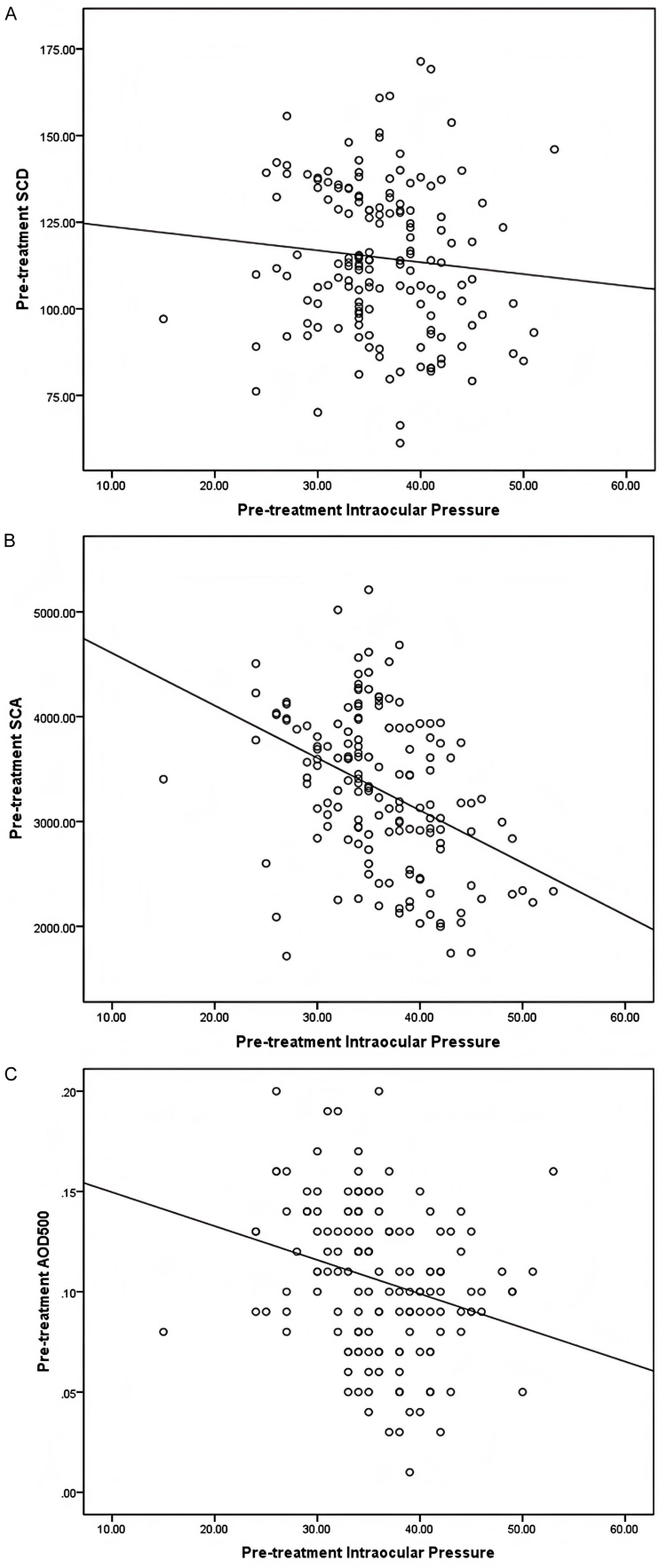

Figure 4. Correlation analysis between IOP and SS-OCT parameters. A: Correlation of IOP with SCD; B: Correlation of IOP with SCA; C: Correlation of IOP with AOD500. Pearson correlation analysis revealed that preoperative IOP was significantly negatively correlated with SCD, SCA, and AOD500 (r = -0.208, -0.402, -0.268; $P < 0.05$), indicating that elevated IOP was associated with smaller SCD and anterior chamber angle opening. IOP: intraocular pressure; SS-OCT: swept-source optical coherence tomography; SCD: Schlemm's canal diameter; SCA: Schlemm's canal area; AOD500: angle opening distance at 500 μm.

edema, chronic inflammation, secondary glaucoma, optic disc edema, or the need for reoperation. All early postoperative adverse reactions had completely resolved, and no new events were observed. Notably, the incidence of adverse reactions at 1 year postoperatively was not higher in the uncontrolled group compared with the controlled group, suggesting that poor postoperative IOP control was caused by complications but was mainly related to insufficient recovery of anterior chamber angle structures (such as SCD, SCA, and AOD500).

Discussion

PACG is a type of glaucoma caused by peripheral iris obstruction of the trabecular meshwork, leading to impaired aqueous humor outflow and angle closure, resulting in elevated IOP. Clinical symptoms of PACG in the prodromal stage include blurred vision, mild ocular distension, and iridization. Patients in the acute attack phase present with severe ocular pain, visual impairment, ipsilateral migraine, and periorbital pain, while in the chronic phase, the cornea ge-

Table 3. Analysis of factors influencing postoperative IOP control in PACG patients

Factors	*B*	*SE*	*Wald*	*P*	*OR*	95% CI
IOP	0.271	0.084	10.404	0.001	1.311	1.112-1.546
SCD	-0.036	0.016	4.816	0.028	0.965	0.935-0.996
SCA	-0.004	0.001	39.814	< 0.001	0.996	0.995-0.998
AOD500	-1.705	0.472	13.019	< 0.001	0.182	0.072-0.459
Constant	2.981	0.658	20.554	< 0.001	19.706	-

Note: IOP: intraocular pressure; PACG: primary angle-closure glaucoma; SCD: Schlemm's canal diameter; SCA: Schlemm's canal area; AOD500: angle opening distance at 500 μm.

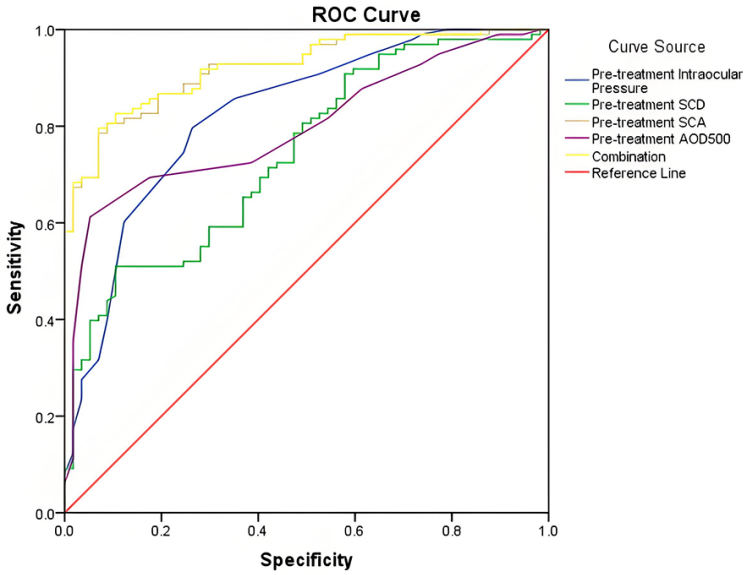

Figure 5. ROC curves of preoperative parameters for predicting postoperative IOP control. This figure illustrates the ROC curves for preoperative IOP, SCD, SCA, AOD500, and the combined multi-parameter model. SCA exhibited the highest AUC (0.921), indicating the strongest predictive ability. The combined model achieved an AUC of 0.923, outperforming any single parameter. ROC: receiver operator characteristic; IOP: intraocular pressure; SCD: Schlemm's canal diameter; SCA: Schlemm's canal area; AOD500: angle opening distance at 500 μm.

nerally regains transparency, but IOP remains persistently elevated [10, 11]. Elevated IOP is the primary risk factor for PACG, and reducing IOP remains the sole definitive intervention to effectively inhibit disease progression. Phaco-GSL is a commonly used surgical approach for PACG, facilitating the elimination of pupillary block and restoring aqueous humor outflow, thereby aiding in IOP control and preserving the optic nerve [12]. The results of this study demonstrate that phaco-GSL effectively improved the morphological characteristics of SC in PACG patients and reduced IOP levels. However, follow-up revealed that the IOP uncontrolled rate was 36.77%. These findings suggest that while this surgical approach is highly feasible, therapeutic efficacy remains suboptimal in some patients. Therefore, this study aimed to identify factors influencing surgical outcomes in PACG patients, providing evidence for enhancing visual acuity control.

Anterior segment OCT provides clear images of the anterior chamber angle, sclera, cornea, and other structures, which is widely used in the imaging of ocular surface morphology, refractive surgery, glaucoma, dry eye, and corneal contact lens-related diseases [13-15]. SS-OCT is an OCT technology based on a swept-source laser, enabling high-resolution, high-speed imaging of biological tissues, which reflects the structural and blood flow characteristics in patients with ophthalmic diseases by measuring data such as RNFL thickness and optic disc parameters [16-18]. RNFL is composed of ganglion cell axons and maintains the physiological functions of the choroid and retina. Lee et al. [19] reported that the presence of paracentral scotomas in visual field testing indicated localized retinal ganglion cell loss. This finding demonstrates that RNFL thinning is a sensitive indicator for PACG-related ocular damage, with its changes preceding both optic disc and visual field damage. Given the key role of RNFL thickness changes in the early diagnosis and disease monitoring of glaucoma, it is crucial to accurately and reliably detect RNFL thickness. In a multicenter cross-sectional study, Song et al. [20] reported that SS-OCT technology enabled the assessment of RNFL thickness in glaucoma patients and enhanced the detection rate of high myopia-associated glaucoma. This study showed that in the uncontrolled group, both global and sectoral RNFL thickness decreased significantly after treatment, whereas RNFL thickness in the

controlled group remained relative stable between before and after treatment measurements. This differential change in RNFL suggests that patients with poor postoperative IOP control are more prone to progressive optic nerve fiber layer damage, whereas those with well-controlled IOP exhibit greater stability in nerve fiber structure. This phenomenon may be attributed to two factors: (1) Prolonged high levels of IOP induce retinal and choroidal hypoxia, leading to morphological alterations in retinal ganglion cell axons and subsequently reducing RNFL thickness [21]. (2) From an anatomical perspective, programmed cell death of retinal ganglion cells persists following PACG. However, in cases with effective IOP control, the apoptosis rate is significantly reduced, thereby stabilizing RNFL thickness or even facilitating partial recovery [4].

The optic disc consists of blood vessels, nerves, and connective tissue, serving as the convergence point for retinal nerve fibers. Bekkers et al. [22] reported a significant reduction in blood flow index and density in the optic disc, peripapillary region, and macular area of glaucoma patients. The present study showed that patients with poor postoperative IOP control exhibited poorer recovery of optic disc structure. The C/D ratio and related structural indicators showed limited postoperative improvement with persisted signs of damage, suggesting insufficient structural reconstruction of the optic nerve. In contrast, patients with well-controlled IOP exhibited more pronounced improvements in optic disc parameters, suggesting that effective IOP control facilitates the recovery of optic nerve morphology. The underlying mechanism is hypothesized to be toxins released from early-stage nerve fiber edema or retinal neuronal damage, which induces degenerative changes in ganglion cells, ultimately leading to their apoptosis [23]. As RNFL thickness gradually decreases, RA declines accordingly, and the C/D ratio continuously increases.

The findings of the present study are, to some extent, consistent with the findings of He et al. [4] and Song et al. [20], who reported that phaco-GSL significantly improved the SC morphology and reduced postoperative IOP in patients with PACG. However, unlike the study by Zhou et al. [12], which mainly focused on short-term follow-up, the present study, based on one-year follow-up results, found through SS-OCT quantitative analysis that the extent of improvement in SCD and SCA was significantly correlated with postoperative IOP control, suggesting that this technique has higher predictive value in long-term efficacy assessment.

In addition, Lee et al. [19] highlighted that RNFL thickness can be used as a sensitive indicator of early glaucomatous damage, and our findings further verified its predictive value. It is worth noting that although some studies [22, 23] reported a linear association between SC morphology and IOP, our study found that the decrease in IOP tended to stabilize once the SCD and SCA recovered to a certain threshold, indicating a plateau phase in postoperative structural remodeling. These differences may be related to the extent of preoperative angle adhesions, the degree of intraoperative separation, and individual differences in angle anatomy, and also reflect the unique advantages of SS-OCT in dynamically monitoring postoperative structural reconstruction after PACG.

Research showed [24] that the morphological characteristics of SC in glaucoma patients were mainly characterized by decreased endothelial cells, lumen narrowing or partial occlusion, and basement membrane thickening; these structural alterations collectively impeded aqueous humor outflow, elevated IOP, and consequently damaged the optic nerve. A Chinese study [23] further highlighted significant morphological characteristics differences in the trabecular meshwork-SC between glaucoma patients and healthy individuals, suggesting that SC morphology may hold promise as a novel ocular drug target. Our study showed that both groups of patients exhibited varying degrees of postoperative recovery in anterior chamber angle structure. However, patients with well-controlled IOP showed more significant improvements in SC and angle opening (SCD, SCA, TIA500, and AOD500). This suggests that phaco-GSL not only helps relieve angle obstruction but also relies heavily on the effective postoperative reconstruction of the anterior chamber angle. Moreover, elevated preoperative IOP was negatively correlated with poorer angle structure parameters. In contrast, better postoperative recovery of anterior chamber angle (as evidenced by increased SCD, SCA, and AOD500) served as a protective factor for well-controlled IOP. This indicates that angle

morphology parameters obtained through SS-OCT can better reflect aqueous humor outflow status and may have certain value in assessing postoperative IOP control outcomes and guiding long-term patient management. A prospective cross-sectional study [24] demonstrated that SS-OCT measurements of SCD and SCA parameters effectively differentiated between acute and chronic PACG, and multiple linear regression analysis found that after phaco-GSL, the IOP of patients decreased, while the changes in SCD and SCA increased, which was consistent with the change trend before and after surgery in this study.

The multivariate analysis in this study revealed that elevated preoperative IOP was an independent risk factor for poor postoperative IOP control, while increases in SC and angle structure parameters (SCD, SCA and AOD500) were associated with better postoperative IOP control, suggesting that the reconstruction of the anterior chamber angle structure is of crucial significance in long-term efficacy. Among these, AOD500 remained in the final model after standardization, with both its regression coefficient and OR value demonstrating stability. This further indicates that anterior chamber angle opening is an important structural parameter influencing postoperative IOP control. These findings suggest that quantitative anterior chamber angle parameters obtained via SS-OCT can serve as reliable indicators for postoperative follow-up and prognostic assessment.

Furthermore, predictive analysis indicated that IOP had strong discriminatory ability in assessing postoperative IOP control. The ROC curve analysis in this study revealed that the AUC values for preoperative IOP, SCD, SCA, and AOD500 were all significantly greater than 0.7, indicating that these structural parameters possessed good predictive capability. Among the parameters, SCA exhibited the highest AUC (0.921), representing the most discriminative single predictor. The multi-parameter combined model achieved an AUC of 0.923, indicating that the combined prediction outperformed any single parameter. This finding highlights the critical role of multivariable analysis in clinical prediction and demonstrates that predictive model integrating risk and protective factors has higher accuracy and clinical utility, providing a more reliable risk assessment tool for postoperative management.

Research limitations and prospects

This study systematically evaluated the application value of the SS-OCT scoring system in quantifying postoperative IOP control in PACG patients and analyzed the dynamic changes of posterior segment RNFL thickness and optic disc parameters, and anterior segment key structures in PACG patients after surgery. Furthermore, the study verified the mechanism by which the SS-OCT scoring system can effectively predict postoperative IOP control, which helps clinicians screen high-risk groups with poor postoperative IOP control and formulate targeted preventive measures in advance, thereby providing a powerful quantitative tool for individualized postoperative management and intervention.

This study does have certain limitations. First, this is a single-center retrospective analysis with a relatively small sample size, which may affect the generalizability of the results. Second, the postoperative follow-up period was only one year, and long-term changes in the anterior chamber angle structure and function remained to be observed. Third, although SS-OCT provides high-resolution imaging of the anterior chamber angle and SC, its quantitative measurement results may be affected by image quality and operational differences.

Further multicenter, prospective studies with larger sample sizes and extended follow-up periods should be conducted to validate the findings of this study. Furthermore, aqueous humor outflow function testing should be integrated with visual field progression assessment to further explore the relationship between angle reconstruction and IOP control following PACG from both structural and functional perspectives.

Conclusion

The SS-OCT scoring system enables precise quantification of postoperative IOP control, RNFL thickness, optic disc parameters, and visual function changes in patients with PACG, providing robust guidance for personalized treatment. Preoperative IOP, SCD, SCA, and AOD500 are critical factors of postoperative

IOP control. This technology holds significant clinical value in long-term efficacy assessment, aiding in disease progression prediction and optimization of glaucoma management strategies.

Disclosure of conflict of interest

None.

Address correspondence to: Huaifeng Li, Department of Ophthalmology Ward 2, Liuyang Jili Hospital, No. 434 Jinsha North Road, Liuyang City, Changsha 410300, Hunan, China. Tel: +86-15974142367; E-mail: 13787140660@163.com

References

[1] Song Y, Zhang H, Zhang Y, Tang G, Wan KH, Lee JWY, Congdon N, Zhang M, He M, Tham CC, Leung CKS, Weinreb RN, Lam DSC and Zhang X. Minimally invasive glaucoma surgery in primary angle-closure glaucoma. Asia Pac J Ophthalmol (Phila) 2022; 11: 460-469.

[2] Zhang N, Wang J, Chen B, Li Y and Jiang B. Prevalence of primary angle closure glaucoma in the last 20 years: a meta-analysis and systematic review. Front Med (Lausanne) 2021; 7: 624179.

[3] Song Y, Lin F, Lv A, Zhang Y, Lu L, Xie L, Tang G, Yuan H, Yang Y, Xu J, Lu P, Xiao M, Zhu X, Yan X, Song W, Li X, Zhang H, Li F, Wang Z, Jin L, Gao X, Liang X, Zhou M, Zhao X, Zhang Y, Chen W, Wang N, Tham CC, Barton K, Park KH, Aung T, Weinreb RN, Tang L, Fan S, Lam DSC and Zhang X; PVP Study group. Phacogoniotomy versus phacotrabeculectomy for advanced primary angle-closure glaucoma with cataract: a randomized non-inferiority trial. Asia Pac J Ophthalmol (Phila) 2024; 13: 100033.

[4] He Y, Zhang R, Zhang C, Jia J, Liu H, He B, Quan Z and Zhang J. Clinical outcome of phacoemulsification combined with intraocular lens implantation for primary angle closure/glaucoma (PAC/PACG) with cataract. Am J Transl Res 2021; 13: 13498-13507.

[5] Yang G, Li K, Yao J, Chang S, He C, Lu F, Wang X and Wang Z. Automatic measurement of anterior chamber angle parameters in AS-OCT images using deep learning. Biomed Opt Express 2023; 14: 1378-1392.

[6] Yazdani S, Naderi Beni A and Pakravan M. Laminar and prelaminar tissue characteristics of glaucomatous eyes using enhanced depth imaging OCT. Ophthalmol Glaucoma 2021; 4: 95-101.

[7] Yeu E, Berdahl JP, Gupta PK and Patterson M. Sensitivity and specificity of SS-OCT for detecting macular pathologies vs SD-OCT. J Cataract Refract Surg 2024; 50: 481-485.

[8] Vounotrypidis E, Haralanova V, Muth DR, Wertheimer C, Shajari M, Wolf A, Priglinger S and Mayer WJ. Accuracy of SS-OCT biometry compared with partial coherence interferometry biometry for combined phacovitrectomy with internal limiting membrane peeling. J Cataract Refract Surg 2019; 45: 48-53.

[9] Group; G, Ophthalmology; So and Association; CM. Expert Consensus on Diagnosis and Treatment of Primary Glaucoma in China (2014). Chinese Journal of Ophthalmology 2014; 50: 382-383.

[10] Li C, Guo C, Yang Y, Yu M, Ge J and Fan Z. Newly Onset Optic Disc Pit Maculopathy (ODP-M) in a patient with Primary Angle-closure Glaucoma (PACG) after surgical iridectomy: a case report. J Glaucoma 2020; 29: e44-e49.

[11] Hu T, Xu L, Chen X, Liu B and Zhang H. Visual acuity and visual field changes in patients with end-stage PACG with tubular visual field after cataract surgery. Ophthalmic Res 2023; 66: 620-626.

[12] Zhou WS, Lin WX, Geng YY and Wang T. Combined phacoemulsification and goniosynechialysis with or without endoscopic cyclophotocoagulation in the treatment of PACG with cataract. Int J Ophthalmol 2020; 13: 1385-1390.

[13] Miguel A, Silva A, Barbosa-Breda J, Azevedo L, Abdulrahman A, Hereth E, Abegão Pinto L, Lachkar Y and Stalmans I. OCT-angiography detects longitudinal microvascular changes in glaucoma: a systematic review. Br J Ophthalmol 2022; 106: 667-675.

[14] Vaz PG, Brea LS, Silva VB, van Eijgen J, Stalmans I, Cardoso J, van Walsum T, Klein S, Barbosa Breda J and Andrade De Jesus D. Retinal OCT speckle as a biomarker for glaucoma diagnosis and staging. Comput Med Imaging Graph 2023; 108: 102256.

[15] Wu JH, Moghimi S, Nishida T, Mohammadzadeh V, Kamalipour A, Zangwill LM and Weinreb RN. Association of macular OCT and OCTA parameters with visual acuity in glaucoma. Br J Ophthalmol 2023; 107: 1652-1657.

[16] Hood DC, La Bruna S, Durbin M, Lee C, Guzman A, Gebhardt T, Wang Y, Stowman AL, De Moraes CG, Chaglasian M and Tsamis E. A pattern-based OCT metric for glaucoma detection. Transl Vis Sci Technol 2024; 13: 21.

[17] García G, Del Amor R, Colomer A, Verdú-Monedero R, Morales-Sánchez J and Naranjo V. Circumpapillary OCT-focused hybrid learning for glaucoma grading using tailored prototypical neural networks. Artif Intell Med 2021; 118: 102132.

[18] Takusagawa HL, Hoguet A, Junk AK, Nouri-Mahdavi K, Radhakrishnan S and Chen TC. Swept-source OCT for evaluating the lamina cribrosa: a report by the american academy of ophthalmology. Ophthalmology 2019; 126: 1315-1323.
[19] Lee JWY, Woo TTY, Yau GSK, Yip S, Yick DWF, Wong J, Wong RLM and Wong IYH. Cross-sectional study of the retinal nerve fiber layer thickness at 7 years after an acute episode of unilateral primary acute angle closure. Medicine (Baltimore) 2015; 94: e391.
[20] Song Y, Li F, Chong RS, Wang W, Ran AR, Lin F, Wang P, Wang Z, Jiang J, Kong K, Jin L, Chen M, Sun J, Wang D, Tham CC, Lam DSC, Zangwill LM, Weinreb RN, Aung T, Jonas JB, Ohno-Matsui K, Cheng CY, Bressler NM, Sun X, Cheung CY, Chen S and Zhang X; Glaucoma Suspects with High Myopia Study Group. High myopia normative database of peripapillary retinal nerve fiber layer thickness to detect myopic glaucoma in a chinese population. Ophthalmology 2023; 130: 1279-1289.
[21] Swaminathan SS, Jammal AA, Berchuck SI and Medeiros FA. Rapid initial OCT RNFL thinning is predictive of faster visual field loss during extended follow-up in glaucoma. Am J Ophthalmol 2021; 229: 100-107.
[22] Bekkers A, Borren N, Ederveen V, Fokkinga E, Andrade De Jesus D, Sánchez Brea L, Klein S, van Walsum T, Barbosa-Breda J and Stalmans I. Microvascular damage assessed by optical coherence tomography angiography for glaucoma diagnosis: a systematic review of the most discriminative regions. Acta Ophthalmol 2020; 98: 537-558.
[23] Tan L, Ma D, He J, Wang H, Chen S and Lin Y. The topographic relationship between choroidal microvascular dropout and glaucomatous damage in primary angle-closure glaucoma. Transl Vis Sci Technol 2022; 11: 20.
[24] Ahmed IIK, De Francesco T, Rhee D, McCabe C, Flowers B, Gazzard G, Samuelson TW and Singh K; HORIZON Investigators. Long-term outcomes from the HORIZON randomized trial for a Schlemm's canal microstent in combination cataract and glaucoma surgery. Ophthalmology 2022; 129: 742-751.